Green and Sustainable Chemistry, 2014, 4, 120-132
Published Online August 2014 in SciRes. http://www.scirp.org/journal/gsc
http://dx.doi.org/10.4236/gsc.2014.43017

Scientific Research

TiO_2 Films Synthesis over Polypropylene by Sol-Gel Assisted with Hydrothermal Treatment for the Photocatalytic Propane Degradation

Vanessa Guzmán-Velderrain, Yudith Ortega López, Jesús Salinas Gutiérrez, Alejandro López Ortiz, Virginia H. Collins-Martínez*

Centro de Investigación en Materiales Avanzados S. C., Laboratorio Nacional de Nanotecnología, Depto. de Materiales Nanoestructurados, Chihuahua, México
Email: *virginia.collins@cimav.edu.mx

Received 24 May 2014; revised 24 June 2014; accepted 24 July 2014

Abstract

The present investigation shows experimental results obtained with TiO_2 thin films synthesized by the sol-gel method assisted with hydrothermal treatment over polypropylene, using the dip coating technique. Obtained coatings were characterized through SEM, XRD, UV-Vis and the photocatalytic activity was monitored by GC. According to results, the hydrothermal treatment facilitates the crystallization of the TiO_2 anatase phase, which is present in all synthesized films. Crystal size formed from precursor solutions (estimated by the Scherrer's equation) depends on the time and temperature of the hydrothermal treatment, wherein solution exposed to a higher temperature treatment of 150˚C for 1.5 h (H150/1.5) exhibited a larger crystal size compared to those synthesized at 80˚C for 1.5 h and 3 h (H80/1.5 and H80/3). Sample H150/1.5 over polypropylene resulted in a uniform and crack free coating. This behavior was attributed to the precursor solution being denser than those synthesized at 80˚C. Additionally, the photocatalytic activity of the coatings was evaluated through the degradation of propane. Coating H150/1.5 reached 100% conversion after 3 h of UV light irradiation.

Keywords

TiO_2 Coating, Polypropylene, Propane Photodegradation, Photocatalysis

*Corresponding author.

How to cite this paper: Guzmán-Velderrain, V., López, Y.O., Gutiérrez, J.S., Ortiz, A.L. and Collins-Martínez, V.H. (2014) TiO_2 Films Synthesis over Polypropylene by Sol-Gel Assisted with Hydrothermal Treatment for the Photocatalytic Propane Degradation. *Green and Sustainable Chemistry*, **4**, 120-132. http://dx.doi.org/10.4236/gsc.2014.43017

1. Introduction

Titanium dioxide is a semiconductor material, which exists in three crystalline phases: anatase, brookite and rutile, with the latter being more stable at high temperatures. However, anatase obtained at temperatures near 400˚C [1], is mainly the phase used as a photocatalyst, which is due to its capacity to adsorb water and to generate hydroxyl groups (OH) [2] [3]. Nowadays, scientists are looking for paths to synthesize TiO_2 at low temperatures for applications in solar cells, fuel cells and photocatalytic systems among others. Many photocatalytic applications are hydrogen production through the splitting of the water molecule, generation of anti-fogging surfaces and remediation treatment for water and air through decomposition of contaminants (mainly organic compounds) [4]. For such treatments, the TiO_2 generally can be applied in a powder form, leading to the need of a recovery process, which in most cases increases the cost of treatment; therefore a practical solution to this problem could be through immobilization of the photocatalyst [5] [6]. One method to immobilize this photocatalyst, is by depositing thin films over suitable substrates such as glass, metals, ceramics or polymers [7]. Polymers are materials, which are characterized by essential properties such as electric insulators, high corrosion, acid, alkaline and solvent resistance. Currently, they are good candidates for industrial applications, like building materials due to their lightness and low cost. However, they present low thermal stability.

Considering polymers as substrates for the TiO_2 thin films and their poor thermal resistance, there is the need to find a suitable synthesis for obtaining crystalline coatings with good adhesion to the substrate, thus avoiding the exposure of these materials to a heat treatment that would eventually degrade the polymer.

There are several film synthesis techniques such as sputtering, pulsed laser deposition, molecular-beam epitaxy, chemical vapor deposition and sol-gel. However, one of the most widely used process is the sol-gel method due to its reproducibility, low temperature processing, small particle size and morphological control, better homogeneity and phase purity compared to traditional ceramic methods, and high efficiency [8]-[10]. Among some disadvantages of this technique, include long preparation times due to the number of processing steps (hydrolysis, polymerization, gelation, condensation, drying and densification); raw materials for this process are expensive (in the case of metal alkoxides); products would present high carbon content when organic reagents are used during the synthesis steps and this would inhibit densification [11].

Sol-gel technique consists in the hydrolysis and condensation of an alkoxide to form a gel at room temperature. When a coating is needed, this gel can be applied to a substrate by several techniques such as spraying (spray coating), rotation (spin coating) or immersion (dip coating) [12].

Moreover, the gel drying process may lead to an amorphous solid. In order to transform this amorphous solid into a crystalline material, an additional step is required, which can be either an aging process or a thermal treatment. On one hand, if aging is used then this step becomes a slow and time-consuming process [13]. On the other hand, if a heat treatment is applied, a powder material can be obtained.

In the present work, in order to accelerate the crystallization process of the TiO_2 gel a hydrothermal treatment is proposed, which allows to obtain materials with a high degree of crystallinity at low temperatures, short times, and with solid micro and macro-porosity. Nam *et al.*, who obtained TiO_2 in anatase phase at low temperatures [14], reported this hydrothermal treatment.

Since, it is intended to obtain a TiO_2 anatase phase film over polymeric substrates (polypropylene). The use of a hydrothermal treatment of the gel before being applied to the substrate becomes of vital importance, because this material cannot be exposed to a heat treatment, due to its low thermal resistance. Therefore, the aim of the present research is to obtain photocatalytic films through sol-gel assisted by hydrothermal treatment on a polypropylene substrate for the degradation of propane as a model molecule under UV light. Additionally, to find optimal conditions to which hydrothermal treatment provides a uniform and cracks free crystalline film with photocatalytic properties.

2. Materials and Methods

2.1. Preparation of the Substrate

Polypropylene (PP, Georg Fischer brand) was used as support for the coatings, since this polymer is commonly employed in industrial applications; furthermore, it is inexpensive and presents excellent chemical and mechanical properties.

PP coated plaques of 1.5 cm wide and 2.7 cm long were employed to carry out the coating characterization, while 20.5 cm long PP coated tubes were used for the photocatalytic evaluation. Previously, both plaques and

tubes were washed with commercial degreaser and rinsed several times with distilled water in order to remove any contaminants. They were allowed to dry at room temperature to then be coated by the dipping (plaques and tubes) technique.

2.2. Preparation of Precursor Solutions

Coating precursor solutions were obtained by sol-gel and prepared by modifying the synthesis proposed by Sheng, Y., *et al*. [15], who used nitric acid as catalyst and ethanol as solvent. For the preparation of the precursor solution; distilled water, isopropanol (JT Baker) and titanium tetraisopropoxide (TTIP) 97% (Aldrich) were mixed in a 1.5/1.5/150 molar ratio, respectively. Acetic acid (JT Baker) was used as a catalyst by adjusting the pH of the solution between 1 and 2. The obtained solution was exposed to a hydrothermal treatment in a Teflon vessel stainless steel autoclave, in order to evaluate four operating conditions.

Two temperatures (80˚C and 150˚C) and two times (1.5 and 3 h) were employed with the objective of finding suitable treatment conditions and best coating physical and chemical features (**Table 1**). Other temperatures and times will be studied aiming to find optimal conditions in a future work. Different hydrothermal treatment conditions were established to produce easy to apply solutions to generate crystalline, uniform and defect free coatings on the polymeric substrate, in addition to maintain photocatalytic activity for the degradation of propane. Coating application was carried out at room temperature using a dip coating device equipped with an immersion and extraction speed control, this speed was fixed to 7.5 cm·min^{-1} with a residence time of 30 s.

2.3. Characterization

Synthesized coatings were peeled off and the loose films were analyzed using an X-ray diffractometer PANalytical with a 2θ diffraction angle from 15˚ to 85˚, with a 0.05˚ step size to examine their crystal structure. Finally, data was analyzed using the Diffrac-Plus package (Bruker AX Systems), and PDF-2 (ICDD, 2002) ICDD PDF-2 database. The crystal size was determined through the Scherrer's equation using the characteristic peak of the obtained diffractograms. The distribution of the film on the substrate was analyzed through the use of a scanning electron microscope (SEM) JEOL, JSM-5800-LV, equipped with an energy dispersive spectroscopy (EDS) system for the elemental analysis of the samples. The light absorption spectra were obtained with a UV-Vis spectrophotometer Perkin Elmer (lambda-10) using an electromagnetic radiation from the visible (Vis) to the near ultraviolet (UV) region. Surface area and porous structure of the samples were evaluated through the nitrogen adsorption isotherms by the Brunauer-Emmett-Teller (BET) technique using a Quantachrome Autosorb 1. Thermogravimetric analyses (TGA) were performed to determine the residual carbon content in the films using a TA Instruments Q500 Thermogravimetric Analyzer, under air atmosphere and heating rate of 10˚C·min^{-1} from 25˚C to 700˚C.

2.4. Photocatalytic Degradation

Photocatalytic evaluation of the synthesized TiO_2 coatings was carried out in a batch type reactor, which consisted of a PP tube with the inner surface coated by the precursor solutions. Irradiation source was a 8W black light lamp (Lumination brand), with a maximum wavelength centered at 365 nm, and dimensions of 26.5 cm long and 1.5 cm wide, and placed in the interior of a 20.5 (length) by 2 cm (inner diameter) polypropylene tube as shown in **Figure 1**. Evaluation time was of 4 h, with gas sampling intervals of 0.25 h. The void volume inside of the tube was of 44.8 cm^3 that represented the distance between the tube wall and lamp (0.5 cm).

For the photocatalytic degradation tests, propane was used as a model molecule with an initial concentration of 20 ppm. Initial gas mixture (propane/atmospheric air) and photocatalytic reaction products were analyzed by a gas chromatograph (GC) using a Clarus Perkin Elmer model 500 equipped with a thermal conductivity detec-

Table 1. Sample identification of the sol-gel assisted hydrothermal treatment coatings.

Sample	Time (h)	Temperature ˚C
H80/1.5	1.5	80
H80/3.0	3.0	80
H150/1.5	1.5	150
H150/3.0	3.0	150

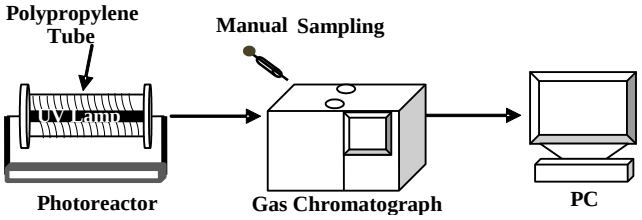

Figure 1. Experimental setup employed for the photocatalytic evaluation of the coatings.

tor (TCD). The gas separation was performed using a column packed Porapak Q. Conditions used for GC analysis were: initial and final oven temperature of 100˚C and 240˚C, respectively under a heating rate of 20˚C·min^{-1}, with an injector and detector temperature of 250˚C. Helium was used as a carrier gas with a flow rate of 30 cm^3·min^{-1}.

3. Results and Discussion

Evaluation and characterization of H150/3 coating was not reported in this paper because after the hydrothermal treatment of this sample the precursor solution from the sol-gel precipitated in such a way that did not allow the formation of a coating on the polypropylene substrate.

3.1. X-Ray Diffraction (XRD)

X-ray diffraction (XRD) was employed as a useful method for structural and microstructural characterizations: diffraction patterns and crystallite size of synthetized TiO_2 thin films.

Figure 2 shows XRD patterns of the synthesized samples (H80/1.5, H80/3 and H150/1.5) and TiO_2 P25. Here, it can be observed that the diffraction patterns of the synthesized samples compared to the diffraction pattern of TiO_2 P25 present only the anatase phase (reflection 101), this pattern was identified by the crystallographic card number 96-900-8215, whereas P25 TiO_2 presents both the anatase and rutile phases. The resulted pure anatase phase of the synthesized samples is attributed to the acetic acid employed during the synthesis, since this produces different complexes with titanium tetraisopropoxide, which provide a control of the condensation speed, thus inducing nucleation in the anatase phase as reported by Parra, R., *et al*. [16].

Moreover, it can be observed that the peak (101) from anatase phase becomes broader as both hydrothermal treatment time and temperature increases and this can be interpreted as a crystal size growth. The order from higher to lower crystal size is as follows: H150/1.5 > H80/3 > H80/1.5. This behavior can be explained according to results reported by Jiaguo, Y., *et al*., H. Yang *et al*. and Cong-hua Zhou *et al*. [17]-[19]. They described that during the hydrothermal treatment a dissolution-recrystallization (Ostwald ripening) process occurs causing an increase in crystal size, which is a function of time and temperature. These results were confirmed, using the Scherrer's equation and data from XRD analysis to estimate the crystal size for the different samples and these are reported in **Table 2**.

In this table, it is evident that an increase in temperature from 80˚C to 150˚C, the crystal size of the coating increased from 5 nm (H80/1.5) to ~7 nm (H150/1.5). The same effect was observed with an increase of treatment time. This behavior was also attributed to the Ostwald ripening process, above described.

However, a careful analysis of these XRD sample patterns reveals that some degree of amorphicity remains within the coatings. This behavior can be associated to the fact that hydrolysis and condensation of titanium alkoxides are favored and hydroxide or hydrated oxide precipitates readily occur. The remaining alkoxy groups in the particles then act as structural impurities, avoiding crystallization and therefore, amorphous particles are formed [20]. On the other hand, hydrothermal treatment contributes to enhance crystallization by finishing hydrolysis before condensation may proceed considerably. Furthermore, water acts as promoter for hydrolysis, whereas the acid serves to protonate with a negative charge to the alkoxide groups, facilitating hydrolysis and partly inhibiting condensation, *i.e*., electrostatic repulsion between protonated hydrolyzed particles. Electrostatic repulsion created by charges adsorbed on the particles counteracts the particle agglomeration caused by the attractive van der Waals forces, and then titanium hydrous oxides are formed [20]. During hydrothermal treatment, these hydrous oxides are condensed to form pure oxide clusters, which serve as nucleation centers for the subsequent growth of TiO_2 nanocrystallites.

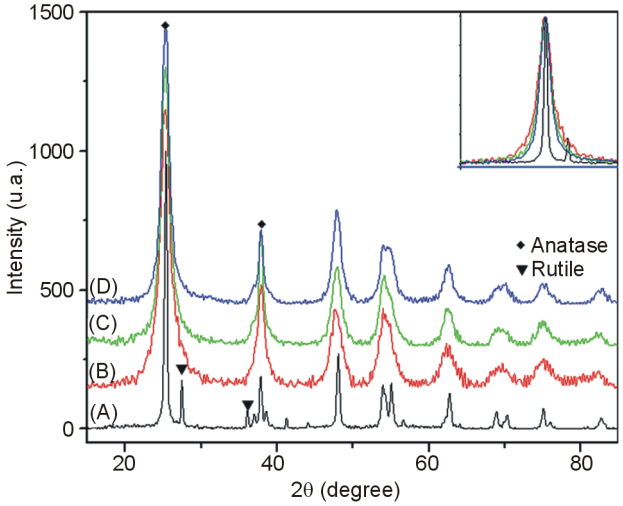

Figure 2. XRD patterns of coatings (A) P25, (B) H80/1.5, (C) H80/3 and (D) H150/1.5.

Table 2. Sample crystal sizes calculated by the Scherrer's equations.

Sample	Crystallite Size (nm)
25	21
H80/1.5	5
H80/3	6.5
H150/1.5	6.8

3.2. Scanning Electron Microscopy (SEM)

In order to perform a detailed study of the basic features that coatings should meet such as morphology, uniformity, homogeneity and chemical composition of the films, they were characterized and analyzed by SEM and EDS, respectively. Since these are determining factors in the properties and performances of the films.

Figure 3 shows SEM images at 100× magnification, where interfaces of the P25 TiO_2 H80/1.5, H80/3 and H150/1.5 coatings are observed. The left portion of the image is related to the area of coated polymer (polypropylene) which is characterized by a lighter shade than the uncoated area (right) which is perceived with a darker shade. At this magnification, the sol-gel/hydrothermal synthesized coatings appear to be continuous and homogeneous compared to the P25 TiO_2 coating, this latter shows material agglomeration onto the substrate. This can be attributed to P25 TiO_2 particles presumably suspended in the solution, which at the time of the dip-coating process were not evenly distributed.

Figure 4 shows micrographs of the coatings at higher magnifications (500×), where they exhibit slight imperfections. For example, sample H80/1.3 present discontinuities and agglomeration of material on the substrate, while H80/3 and H150/1.5 exhibit small fractures within the covered area, and being greater for the H80/3 coating. These fractures (cracks) are attributed to the contractions that occur during drying of the coating process and are due to fast evaporation of water and solvent present in the precursor solution as reported by Vera (2008) [6].

In order to characterize the elemental composition and possible contaminants of the synthesized coatings an SEM-EDS analysis was performed and results are reported in **Table 3**, (TiO_2 P25, H80/1.5, H80/3 and H150/1.5, respectively). In this table, it can be observed that the titanium element (Ti) is present only on the coated area. However, this is found in less amount in the TiO_2 P25 coating (**Table 3**) because this element was not presumably evenly distributed on the polymer surface. For the synthesized coatings, it can be seen that as the hydrothermal-treatment time or temperature increased, the TiO_2 content in the sample also increased, with coating H150/1.5 being this one with the greatest TiO_2 content (**Table 3**). Moreover, the carbon content in the films decreased as the hydrothermal-treatment time or temperature increased. This behavior can be explained according to the studies from Hsiao *et al.* [21]. They reported that during hydrothermal crystallization in an autoclave, the

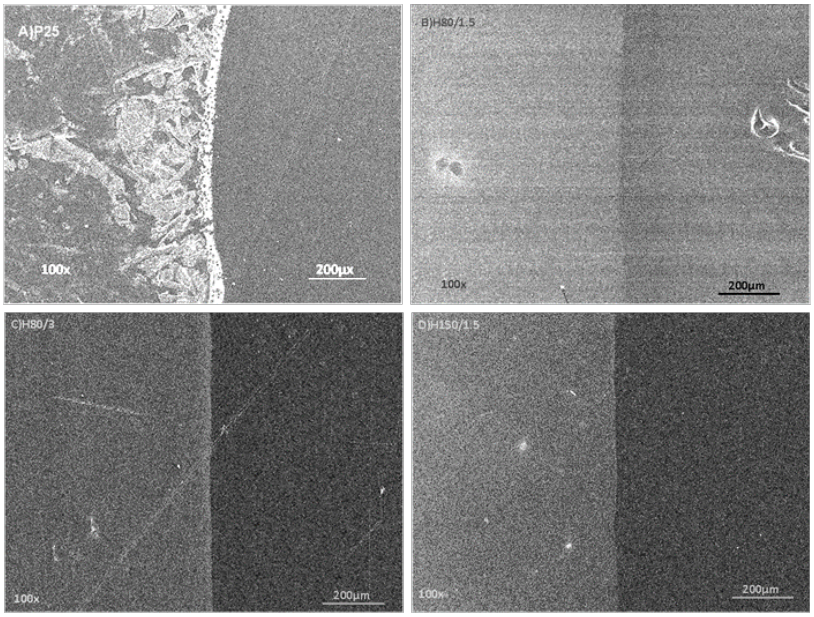

Figure 3. 100× SEM image of coatings interfaces with coated area (left) and uncoated area (right).

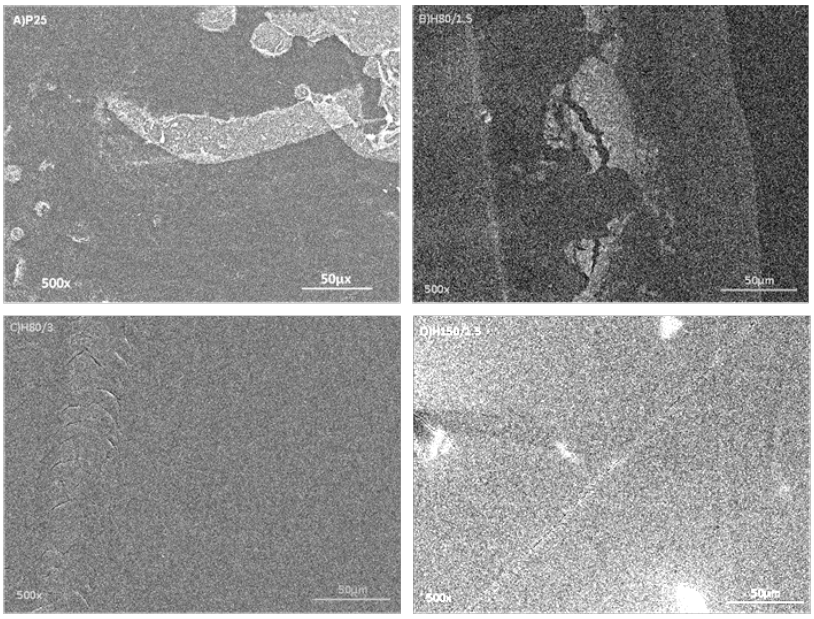

Figure 4. 500× SEM image of the synthesized coatings and P25.

Table 3. Elemental analysis by EDS for coating and P25.

Sample	General Analysis Coated Area %W			General Analysis Uncoated Area %W		
	Ti	O	C	Ti	O	C
P25	2.43	1.36	96.12	0.00	0.65	99.35
H80/1.5	16.54	6.69	76.77	0.00	1.05	98.95
H80/3	17.37	23.65	58.98	0.00	1.59	98.41
H150/1.5	33.21	37.55	29.23	0.00	2.83	97.17

CO_2 generated as byproduct from the alcohol and alkoxide decomposition reactions, caused an increase of the internal pressure and thus producing a reduction of the amount of organic impurities and an enhancement of the material crystallinity. Presumably, these decomposition reactions are the ones that explain the cause to a decrease in the carbon content of the synthesized films, which were exposed to a greater hydrothermal treatment time or temperature.

One of the main issues associated with coatings over polymer substrates is the coating bonding to the substrate. In the particular case of the synthetized coatings in this work, anchoring of these can be attributed to the fact that OH-groups from TiO_2 nanoparticles act as bonding sites via Hydrogen Bridge to polypropylene as claimed by Cerrada *et al*. [22].

Figure 5 describes the synthesis mechanism of the sol-gel process followed by the hydrothermal treatment [23] and finally, the proposed anchoring mechanism of the TiO_2 to polypropylene. In this figure, it can be seen that as a product of the sol-gel (hydrolysis and condensation) process an amorphous material is obtained. Once the hydrothermal treatment is applied to the gel, a crystalline material is reached. In this step, OH groups surround the TiO_2 anatase. Then oxygen atoms from these groups bridge to hydrogen atoms from polypropylene achieving the film cleavage.

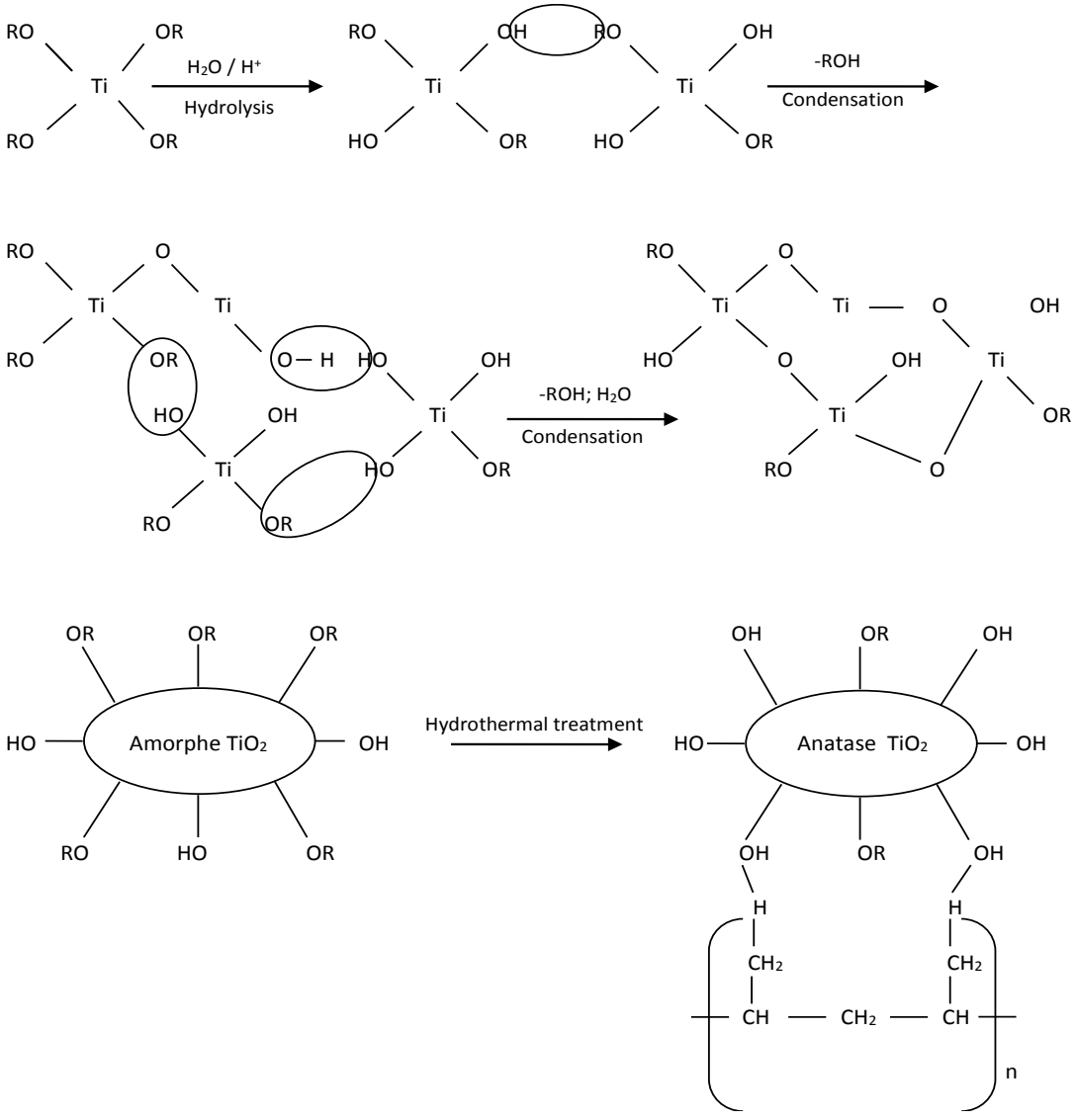

Figure 5. Anchoring mechanism of the TiO_2 on polypropylene and sol-gel mechanism and hydrothermal treatment.

3.3. BET Surface Area

The Brunauer, Emmett and Teller (BET) technique was used with the aim of determining the textural properties of the synthesized coatings. These properties are essential for any catalytic material because their performance is considered a surface phenomenon. For example, the greater the surface area the higher amount of active sites available for the catalytic process (adsorption, chemical reaction and desorption).

Figure 6 shows nitrogen adsorption-desorption isotherms, where it can be observed that coatings H80/1.5, H80/3 and H150/1.5 present a Type IV isotherm that according to the IUPAC classification it corresponds to a multilayer adsorption which characteristic hysteresis is of mesoporous materials. This hysteresis also denotes a type H_2 with inkbottle shape porous [24].

In **Table 4**, it can be seen that coating surface areas are affected with an increase of both time as well as temperature of hydrothermal treatment. A greater temperature and time treatment is reflected in a decrease of surface area. This behavior can be attributed to a growth of crystal size due to the effect of dissolution-recrystallization process above described [18] [19].

3.4. Thermogravimetric Analysis (TGA)

A temperature scan was performed to the synthesized coatings using TGA in order to determine the amount of residual organic material from reagents during the coating synthesis, since these coatings were not subjected to a heat treatment because the material used as substrate (polymer) is not able to withstand high temperature treatments.

TGA results for the synthesized films are presented in **Figure 7**. In this figure, weight loss for synthesized films was observed at 3 different temperature ranges, namely, below 105˚C, at 105˚C - 250˚C and at 250˚C - 450˚C. In the first region (below 105˚C) the weight loss (10.8%, 9.4% and 4.3%, for H80/1.5, H80/3 and 150/1.5, respectively) is thought to result from the evaporation of physically adsorbed water and/or the residual organic solvent as isopropanol. While, the weight loss (16.2%, 15.1% and 9.7%, respectively) at 105˚C - 250˚C

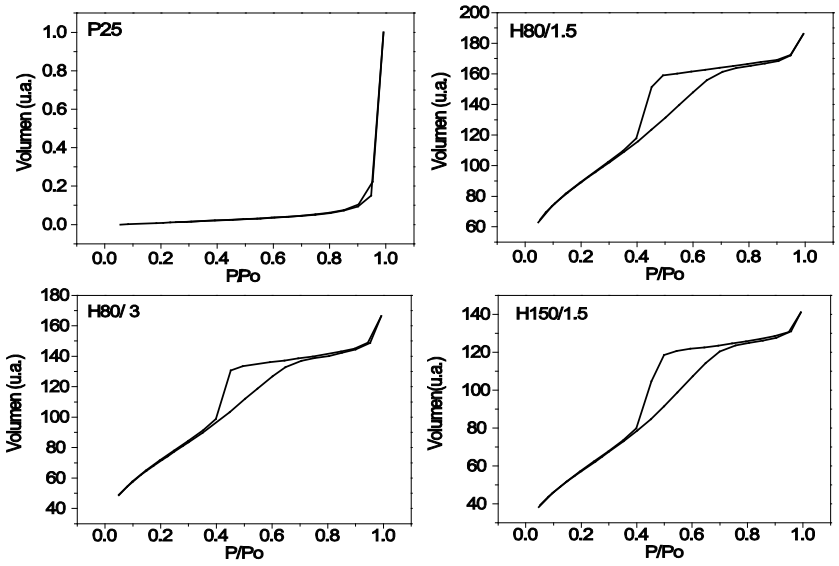

Figure 6. Nitrogen adsorption-desorption isotherms.

Table 4. Surface area by BET.

Sample	BET Area ($m^2 \cdot g^{-1}$)
25	50
H80/1.5	321
H80/3	261
H150/1.5	210

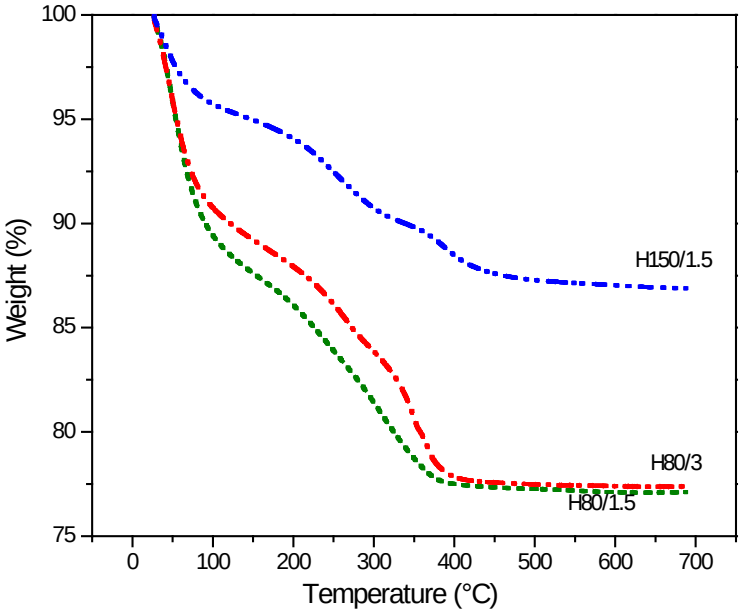

Figure 7. TGA analysis for the synthesized coatings.

is due to the removal of chemisorbed hydroxyl groups [25].

Finally, the weight loss (22.7%, 22.4% and 12.4%, respectively) at 250˚C - 450˚C is attributed to oxidation of the alkoxide groups bonded to the Ti-atom (RO-Ti-O-Ti-OR) as suggested by Sayilkan *et al*. [26], which persist due to incomplete hydrolysis [27]. Because the hydrothermal treatment for crystallization is favored by the generated autogenous pressure (which depends partly on the temperature), it is observed that the sample with the least amount of residual organic material is the one synthesized at a higher hydrothermal temperature. This residual organic content increased with a reduction of both time and hydrothermal treatment temperature, which is the case of the coating synthesized at 80˚C for 1.5 h (H80/1.5).

3.5. UV-VIS Spectroscopy

The fundamental absorption corresponding to electron excitation from the valance to the conduction band can be used to determine the value of the optical band gap (Eg).

Figure 8 shows plots obtained through UV-Vis of the synthesized coatings. This technique was employed in order to investigate the optical properties of the coatings such as the energy of the forbidden band (band gap), since this is determined by the conditions of wavelength or energy at which the film is excited. This value was obtained by the Tauc technique through calculation of the adsorption coefficient (α, Equation (1)):

$$\alpha = (-LNT)/d \tag{1}$$

where T is the value of the transmittance and d the film thickness. Band gap values for each precursor solution are obtained by extrapolation of a straight line where $\alpha = 0$ in the graph $(\alpha h\nu)^{1/2}$ vs. $h\nu$ (energy) [28].

Furthermore, it can be seen in **Figure 8** that the hydrothermal treatment affects the values of the band gap energy (Eg) of the coatings. Results indicate that the lowest value of Eg corresponds to the H150/1.5 coating synthesized at 150˚C and 1.5 h of hydrothermal treatment with a 3.26 eV, followed by H80/3 (3.28 eV) and finally with H80/1.5 (3.43 eV) sample coating. Here, it can be observed that the first two samples (H150/1.5 and H80/3) present values close to those of the anatase, which is 3.2 eV as reported by Kim *et al.* [29] and Carp *et al.* [30]. This Eg lowering effect is attributed to a higher content of crystalline material within the coatings, which is obtained by the hydrothermal treatment at higher temperatures and times. At these conditions, condensation and polymerization reactions are presumably accelerated and enhanced. These reactions can be considered as responsible for the greater crystallization of the samples [31]. Sample H80/1.5 shows the biggest value Eg, which is related with a higher amount of amorphous material contained in this sample. This result agrees with reported values by Prasai *et al.* [32].

3.6. Photocatalytic Activity

Figure 9 shows photocatalytic activity results for coatings H80/1.5, H80/3 (synthesized at 80˚C for 1.5 and 3 h, respectively) and H150/1.5 (synthesized at 150˚C for 1.5 h). In this figure it can be observed that the higher temperature and time treatment, there is an enhancement in the photocatalytic activity, which is related to the degree of crystallinity of the coatings and the amount of organic matter present on their surface. According to the XRD and TGA analyses, the coating with higher crystallinity and less organic material on its surface was the one synthesized at 150˚C for 1.5 h (H150/1.5) which was capable to degrade 100% propane in a period of 3 h. Also in this figure it can be seen that this degradation capacity is smaller for coatings generated from precursor solutions exposed at 80˚C, with 3 and 1.5 h of hydrothermal treatment with conversions of 95 (H80/3) and 89% (H80/1.5), respectively.

Furthermore, in **Figure 9** it is evident that P25 TiO_2 coating exhibited a high and fast propane degradation and this is attributed to the total available surface area being crystalline. However, this coating presents several irregularities as observed by the SEM images, which show that this coating is neither continuous nor homogeneous. Additionally, this discontinuity affects the ease of handling that is accompanied with an ease of detachment (loss of material). Moreover, the coatings generated from the proposed synthesis are continuous and exhibit small amounts of cracks, thereby improving their physical properties and allowing the easy handling of the coated surfaces.

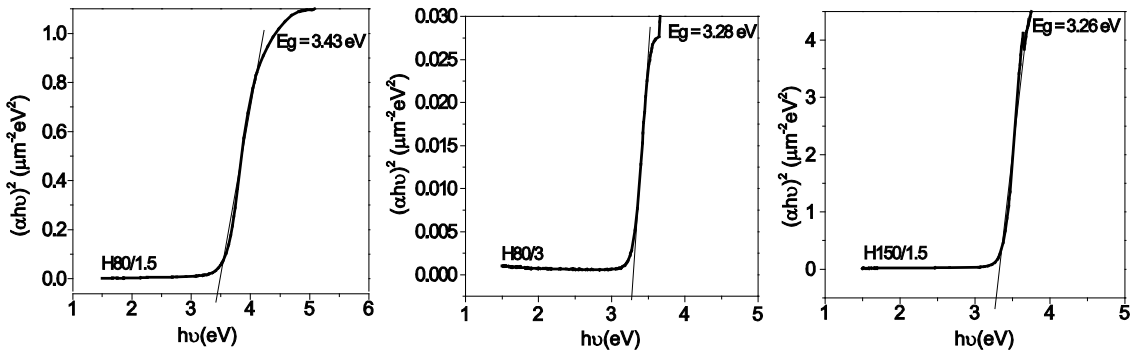

Figure 8. UV-Vis spectra of different coatings.

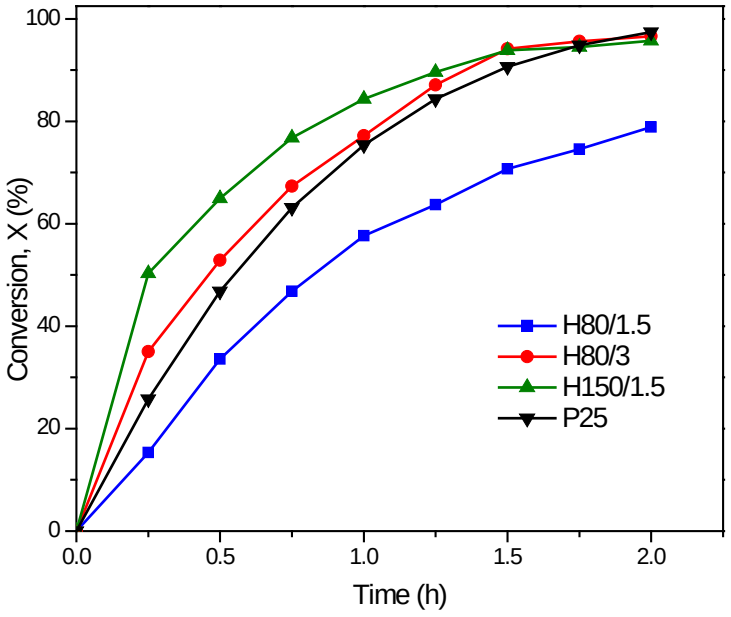

Figure 9. Degradation conversion as function of time for the studied samples.

4. Conclusions

TiO_2 coatings were synthesized in anatase phase by the sol-gel technique assisted by hydrothermal treatment at room temperature and deposited on polypropylene (PP) substrates through the dip-coating technique. The coating synthesized under hydrothermal treatment conditions at 150˚C for 1.5 h was the one that presented a band-gap energy (3.26 eV) closer to the value of pure anatase TiO_2 (3.2 eV). This synthesized coating (H150/1.5) is continuous, with minimal presence of cracks and with the least amount of remaining organic matter (12%), thus allowing a higher photocatalytic activity toward the degradation of propane. The sol-gel followed by hydrothermal treatment provides a better distribution of the coating on the substrate compared to that obtained by the dispersion of TiO_2 P25 particles on the substrate.

Furthermore, the hydrothermal treatment promotes the crystallization of amorphous TiO_2 at low temperatures, while the acetic acid, acting as a catalyst, promotes the formation of the pure anatase phase. The hydrothermal treatment temperature of 150˚C for 1.5 h produces optimal conditions for generating a dense solution that allows coatings to achieve a better distribution over the polymer surface and to generate a uniform film with less cracks. An increase in the hydrothermal treatment temperature and/or time promotes crystal growth that is attributed to the dissolution-recrystallization effect, which results in a reduction of carbonaceous matter within the coating. The coating with the highest crystallinity and less carbonaceous matter (H150/1.5) exhibited the greatest photocatalytic activity among synthesized materials.

Acknowledgements

The authors are grateful to Enrique Torres, Karla Campos and Luis de la Torre for their inputs on results for XRD, SEM and UV-Vis spectroscopy, respectively. In addition, it has to be acknowledged the Centro de Investigación en Materiales Avanzados, S. C. (CIMAV) and Consejo Nacional de Ciencia y Tecnología (CONACYT) for their support in funding and the use of their infrastructure.

References

[1] Arnal, P., Corriu, R., Leclercq, D., Mutin, P. and Vioux, A. (1996) Preparation of Anatase, Brookite and Rutile at Low Temperature by Non Hydrolytic Sol-Gel Methods. *Journal of Materials Chemistry*, **6**, 1925.

[2] Li, W., Ni, C., Shah, S., Lin, H. and Huang, C. (2004) Size Dependence of Thermal Stability of TiO_2 Nanoparticles. *Journal of Applied Physics*, **96**, 6663-6668.

[3] Kääriäinen, M.-L., Kääriäinen, T.O. and Cameron, D.C. (2009) Titanium Dioxide Thin Films, Their Structure and Its Effect on Their Photoactivity and Photocatalytic Properties. *Thin Solid Films*, **517**, 6666-6670. http://dx.doi.org/10.1016/j.tsf.2009.05.001

[4] Ashimoto, K.H., Irie, H. and Fujishima, A. (2005) TiO_2 Photocatalysis: A Historical Overview and Future Prospects. *Japanese Journal of Applied Physics*, **12**, 8269. http://dx.doi.org/10.1143/JJAP.44.8269

[5] Ao, Y., Xu, J., Shen, X. and Yuan, C. (2008) Low Temperature Preparation of Anatase TiO_2-Activated Carbon Composite Films. *Applied Surface Science*, **254**, 4001-4006. http://dx.doi.org/10.1016/j.apsusc.2007.12.026

[6] Vera, M. (2008) Fijación del TiO_2 a sustratos de vidrio por Sol-Gel combinado con TiO_2 comercial. *Proceedings of* 2*do Encuentro de jóvenes investigadores en ciencia y tecnología de materiales* (*SAM*), posadas-Misiones, 16-17 Octubre 2008, 52.

[7] Medina-Valtierra, J., Garcia-Servin, J., Frausto-Reyes, C. and Calixto, S. (2006) The Photocatalytic Application and Regeneration of Anatase Thin Films Whit Embedded Commercial TiO_2 Particles Deposited on Glass Microrods. *Applied Surface Science*, **252**, 3600-3608. http://dx.doi.org/10.1016/j.apsusc.2005.05.045

[8] Reza, E., Reza, M. and Hossein, A. (2014) Sol-Gel Derived Al and Ga Co-Doped ZnO Thin Films: An Optoelectronic Study. *Applied Surface Science*, **290**, 252-259. http://dx.doi.org/10.1016/j.apsusc.2013.11.062

[9] Popa, M., Mereu, R., Filip, M., Gabor, M., Petrisor Jr., T., Ciontea, L. and Petrisor, T. (2013) Highly c-Axis Oriented ZnO Thin Film Using 1-Propanol as Solvent in Sol-Gel Synthesis. *Materials Letters*, **92**, 267-270. http://dx.doi.org/10.1016/j.matlet.2012.10.099

[10] Wang, X., Shi, F., Gao, X., Fan, C., Huang, W. and Feng, X. (2013) A Sol-Gel Dip/Spin Coating Method to Prepare Titanium Oxide Films. *Thin Solid Films*, **548**, 34-39. http://dx.doi.org/10.1016/j.tsf.2013.08.056

[11] Carballo, L. and Galindo, H. (2001) Estudio de los Procesos Sol-gel para la Obtención de un Aglutinante Apropiado para el Peletizado de Alúmina Revista Ingeniería e Investigación No. 48.

[12] Suciu, R., Indrea, E., Silipas, T., Dreve, S., Rosu, M., Popescu, V., Popescu, G. and Nascu, H. (2009) TiO_2 Thin Films

Prepared by Sol-Gel Method. *Journal of Physics Conference Series*, **182**, 1. http://dx.doi.org/10.1088/1742-6596/182/1/012080

[13] Praveen, P., Viruthagiri, G., Mugundan, S. and Shanmugam, N. (2014) Structural, Optical and Morphological Analyses of Pristine Titanium Di-Oxide Nanoparticles Synthesized via Sol-Gel Route. *Spectrochimica Acta Part A*: *Molecular and Biomolecular Spectroscopy*, **117**, 622-629. http://dx.doi.org/10.1016/j.saa.2013.09.037

[14] Nam, W. and Han, G. (2003) A Photocatalytic Performance of TiO_2 Photocatalyst Prepared by the Hydrothermal Method. *Korean Journal of Chemical Engineering*, **20**, 180.

[15] Sheng, Y., Liang, L., Xu, Y. and Wu, D. (2008) Low-Temperature Deposition of the High Performance Anatase-Titania Optical Films via Modified Sol-Gel Route. *Optical Materials*, **30**, 1310-1315. http://dx.doi.org/10.1016/j.optmat.2007.06.010

[16] Parra, R., Góes, M.S., Castro, M.S., Longo, E., Bueno, P.R. and Varela, J.A. (2008) Reaction Pathway to the Synthesis of Anatase via the Chemical Modification of Titanium Isopropoxide with Acetic Acid. *Chemistry of Materials*, **20**, 143-150. http://dx.doi.org/10.1021/cm702286e

[17] Yu, J., Yu, H., Cheng, B., Zhou, M. and Zhao, X. (2006) Enhanced Photocatalytic Activity of TiO_2 Powder (P25) by Hydrothermal Treatment. *Journal of Molecular Catalysis A*: *Chemical*, **253**, 112-118. http://dx.doi.org/10.1016/j.molcata.2006.03.021

[18] Yang, H.G. and Zeng, H.C. (2004) Preparation of Hollow Anatase TiO_2 Nanospheres via Ostwald Ripening. *Journal of Physical Chemistry B*, **108**, 3492-3495. http://dx.doi.org/10.1021/jp0377782

[19] Zhou, C.H., Xu, S., Yang, Y., Yang, B.C., Hu, H., Quan, Z.C., Sebo, B., Chen, B.L., Tai, Q.D., Sun, Z.H. and Zhao, X.Z. (2011) Titanium Dioxide Sols Synthesized by Hydrothermal Methods Using Tetrabutyl Titanate as Starting Material and the Application in Dye Sensitized Solar Cells. *Electrochimica Acta*, **56**, 4308-4314. http://dx.doi.org/10.1016/j.electacta.2011.01.054

[20] Yun, Y., Chung, J., Kim, S., Hahn, S. and Kim, E.J. (2004) Low Temperature Coating of Sol-Gel Anatase Thin Films. *Materials Letters*, **58**, 3703. http://dx.doi.org/10.1016/j.matlet.2004.07.018

[21] Hsiao, P.T., Lu, M.D., Tung, Y.L. and Teng, H. (2010) Influence of Hydrothermal Pressure during Crystallization on the Structure and Electron-Conveying Ability of TiO_2 Colloids for Dye-Sensitized Solar Cells. *Journal of Physical Chemistry C*, **114**, 15625. http://dx.doi.org/10.1021/jp1061013

[22] Cerrada, M., Serrano, C., Sánchez-Chaves, M., Fernández-García, M., Fernandez-Martin, F., de Andrés, A., Jiménez, R., Kubacka, A., Ferrer, M. and Fernández-Garcia, M. (2008) Self-Sterilized EVOH-TiO_2 Nanocomposites: Interface Effects on Biocidal Properties. *Advanced Functional Materials*, **18**, 1949-1960. http://dx.doi.org/10.1002/adfm.200701068

[23] Sayılkan, F., Asiltürk, M., Tatar, P., Kiraz, N., Arpaü, E. and Sayılkan, H. (2007) Preparation of Re-Usable Photocatalytic Filter for Degradation of Malachite Green Dye under UV and vis-Irradiation. *Journal of Hazardous Materials*, **148**, 735-744. http://dx.doi.org/10.1016/j.jhazmat.2007.03.036

[24] He, F., Li, J., Li, T. and Li, G. (2014) Solvothermal Synthesis of Mesoporous TiO_2: The Effect of Morphology, Size and Calcination Progress on Photocatalytic Activity in the Degradation of Gaseous Benzene. *Chemical Engineering Journal*, **237**, 312-321. http://dx.doi.org/10.1016/j.cej.2013.10.028

[25] Murugan, K., Rao, T., Narashima, G.V., Gandhi, A. and Murty, B.S. (2011) Effect of Dehydration Rate on Non-Hydrolytic TiO_2 Thin Film Processing: Structure, Optical and Photocatalytic Performance Studies. *Materials Chemistry & Physics*, **129**, 810-815. http://dx.doi.org/10.1016/j.matchemphys.2011.05.011

[26] Sayilkan, F., Asiltürk, M., Sayilkan, H., Onal, Y., Akarsu, M. and Arpaü, E. (2005) Characterization of TiO_2 Synthesized in Alcohol by Sol-Gel Process: The Effects of Annealing Temperature and Acid Catalyst. *Turkish Journal of Chemistry*, **29**, 697-706.

[27] Bischoff, B.L. and Anderson, M.A. (1995) Peptization Process in the Sol-Gel Preparation of Porous Anatase (TiO_2). *Chemistry of Materials*, **7**, 1772-1778.

[28] Hemissi, M. and Amardjia-Adnani, H. (2007) Optical and Structural Properties of Titanium Oxide Thin Films Prepared by Sol-Gel Method Digest. *Journal of Nanomaterials and Biostructures*, **2**, 299.

[29] Kim, T.K., Lee, M.N., Lee, S.H., Park, Y.C., Jung, C.K. and Boo, J.H. (2005) Development of Surface Coating Technology of TiO_2 Powder and Improvement of Photocatalytic Activity by Surface Modification. *Thin Solid Films*, **475**, 171-177. http://dx.doi.org/10.1016/j.tsf.2004.07.021

[30] Carp, O., Huisman, C.L. and Reller, A. (2004) Photoinduced Reactivity of Titanium Dioxide. *Progress in Solid State Chemistry*, **32**, 33-177. http://dx.doi.org/10.1016/j.progsolidstchem.2004.08.001

[31] Yu, J., Wang, G., Cheng, B. and Zhou, M. (2007) Effects of Hydrothermal Temperature and Time on the Photocatalytic Activity and Microstructures of Bimodal Mesoporous TiO_2 Powders. *Applied Catalysis B*: *Environmenral*, **69**, 171.

[32] Prasai, B., Cai, B., Underwood, M.K., Lewis, J.P. and Drabold, D.A. (2012) Properties of Amorphous and Crystalline Titanium Dioxide from First Principles. *Journal of Materials Science*, **47**, 7515-7521. http://dx.doi.org/10.1007/s10853-012-6439-6

Scientific Research Publishing (SCIRP) is one of the largest Open Access journal publishers. It is currently publishing more than 200 open access, online, peer-reviewed journals covering a wide range of academic disciplines. SCIRP serves the worldwide academic communities and contributes to the progress and application of science with its publication.

Other selected journals from SCIRP are listed as below. Submit your manuscript to us via either submit@scirp.org or Online Submission Portal.